

## RESEARCH ARTICLE

# Endoglycan (PODXL2) is proteolytically processed by ADAM10 (a disintegrin and metalloprotease 10) and controls neurite branching in primary neurons

Hung-En Hsia<sup>1,2</sup> | Johanna Tüshaus<sup>1,2</sup> | Xiao Feng<sup>1,2</sup> | Laura I. Hofmann<sup>1,2</sup> |  
 Benedikt Wefers<sup>1,3</sup> | Denise K. Marciano<sup>4</sup> | Wolfgang Wurst<sup>1,3,5,6</sup> |  
 Stefan F. Lichtenthaler<sup>1,2,5</sup>

<sup>1</sup>German Center for Neurodegenerative Diseases (DZNE), Munich, Germany

<sup>2</sup>Neuroproteomics, School of Medicine, Klinikum rechts der Isar, Technical University of Munich, Munich, Germany

<sup>3</sup>Institute of Developmental Genetics, Helmholtz Center Munich, Neuherberg/Munich, Germany

<sup>4</sup>Departments of Cell Biology and Internal Medicine, University of Texas Southwestern Medical Center, Dallas, TX, USA

<sup>5</sup>Munich Cluster for Systems Neurology (SyNergy), Munich, Germany

<sup>6</sup>Technical University of Munich-Weihenstephan, Neuherberg/Munich, Neuherberg, Germany

## Correspondence

Stefan F. Lichtenthaler, German Center for Neurodegenerative Diseases (DZNE), Feodor-Lynen-Street 17, D-81377 Munich, Germany.  
 Email: Stefan.Lichtenthaler@dzne.de

## Funding information

Deutsche Forschungsgemeinschaft (DFG), Grant/Award Number: EXC 2145 SyNergy- ID 390857198; Bundesministerium für Bildung und Forschung (BMBF), Grant/Award Number: JPND PMG-AD; Foundation for the National Institutes of Health (FNIH), Grant/Award Number: R01DK099478; Deutsche Forschungsgemeinschaft (DFG), Grant/Award Number: FOR2290

## Abstract

Cell adhesion is tightly controlled in multicellular organisms, for example, through proteolytic ectodomain shedding of the adhesion-mediating cell surface transmembrane proteins. In the brain, shedding of cell adhesion proteins is required for nervous system development and function, but the shedding of only a few adhesion proteins has been studied in detail in the mammalian brain. One such adhesion protein is the transmembrane protein endoglycan (PODXL2), which belongs to the CD34-family of highly glycosylated sialomucins. Here, we demonstrate that endoglycan is broadly expressed in the developing mouse brains and is proteolytically shed *in vitro* in mouse neurons and *in vivo* in mouse brains. Endoglycan shedding in primary neurons was mediated by the transmembrane protease a disintegrin and metalloprotease 10 (ADAM10), but not by its homolog ADAM17. Functionally, endoglycan deficiency reduced the branching of neurites extending from primary neurons *in vitro*, whereas deletion of ADAM10 had the opposite effect and increased neurite branching. Taken together, our study discovers a function for endoglycan in neurite branching, establishes endoglycan as an ADAM10 substrate and suggests that ADAM10 cleavage of endoglycan may contribute to neurite branching.

## KEYWORDS

ADAM10, ADAM17, neurite branching, PODXL2, seizure protein 6

**Abbreviations:** ADAM, A disintegrin and metalloprotease; CSF, cerebrospinal fluid; DIV, days *in vitro*; EG, endoglycan; PODXL, podocalyxin; SEZ6, seizure protein 6.

This is an open access article under the terms of the Creative Commons Attribution-NonCommercial License, which permits use, distribution and reproduction in any medium, provided the original work is properly cited and is not used for commercial purposes.

© 2021 The Authors. *The FASEB Journal* published by Wiley Periodicals LLC on behalf of Federation of American Societies for Experimental Biology

## 1 | INTRODUCTION

Ectodomain shedding of membrane proteins is a fundamental mechanism to control the communication between cells and their environment, including in the nervous system.<sup>1</sup> In this process, a protease—referred to as sheddase—cleaves a membrane protein substrate within its extracellular domain (ectodomain) at a site close to the transmembrane domain. This juxtamembrane cleavage results in the release—also referred to as shedding—of the ectodomain from the membrane and in its subsequent secretion, for example into body fluids or into the conditioned medium of cultured cells. A diverse range of mostly membrane-bound proteases, such as ADAMs (A disintegrin and metalloproteases) and BACE ( $\beta$ -site APP cleaving enzyme) proteases (BACE1 and BACE2), mediates shedding of presumably more than 1000 membrane proteins.<sup>1</sup> However, for most sheddases, the substrate spectrum is only partly known.

One major sheddase is the metalloprotease ADAM10 that is ubiquitously expressed and has essential functions in different tissues and organs.<sup>2-4</sup> In the nervous system, ADAM10 is expressed both pre- and post-synaptically<sup>5-12</sup> and has several well-established substrates, where proteolytic cleavage acts as a molecular switch to control substrate function.<sup>13,14</sup> Examples are ADAM10 cleavage of Notch1 during nervous system development,<sup>15-17</sup> processing of death receptor 6 during peripheral myelination<sup>18</sup> and shedding of NrCAM during neurite outgrowth.<sup>19</sup> Shedding of other nervous system substrates through ADAM10 is linked to neurological and psychiatric diseases, such as cleavage of the amyloid precursor protein (APP) and the phagocytic protein TREM2 to Alzheimer's disease,<sup>16,20-26</sup> the prion protein to prion diseases<sup>27</sup> and N-cadherin to Huntington's disease.<sup>28</sup> This makes ADAM10 a potential drug target,<sup>29,30</sup> and a first phase 2 clinical trial with an ADAM10-targeted drug was conducted with 21 Alzheimer's disease patients.<sup>19,31</sup>

In addition to the established substrates, a proteomic study identified numerous additional membrane proteins that require ADAM10 for their normal shedding in primary murine neurons.<sup>32</sup> Although proteomic methods are powerful tools to unbiasedly identify substrate candidates of membrane sheddases,<sup>33</sup> the identified substrate candidates need to be validated by other methods. Moreover, a detailed mechanistic investigation and functional characterization of their ADAM10 cleavage is required to better understand the physiological functions of ADAM10 in the nervous system and for preclinical validation of ADAM10 as a drug target of nervous system disorders.

One of the proteomically identified substrate candidates of ADAM10, that is not yet validated by other methods and further characterized with regard to its proteolytic

processing, is the type I membrane protein endoglycan (also known as PODXL2, podocalyxin-like protein 2<sup>32</sup>). Endoglycan belongs to the CD34 family of sialomucins together with CD34 and podocalyxin (PODXL), which act as cell adhesion proteins.<sup>34</sup> Mouse endoglycan has 603 amino acids, with an N-terminal signal peptide, a long ectodomain of 471 amino acids, a single transmembrane domain and a short cytoplasmic domain of 83 amino acids, according to Uniprot (Figure 1A). The endoglycan ectodomain is highly N- and O-glycosylated, sialylated and chondroitin sulfate-modified and carries one unpaired cysteine which allows endoglycan to form covalent dimers.<sup>35-37</sup> Endoglycan is broadly expressed with high expression levels observed in brain, pancreas, kidney and lymph nodes, based on mRNA expression data.<sup>35</sup> The molecular function of endoglycan is not yet well understood, partly because endoglycan-deficient mice are healthy and without an obvious phenotype.<sup>38</sup> In the immune system endoglycan can act as a cell adhesion protein, because it is a ligand for L-selectin and may contribute to lymphocyte homing.<sup>36,37,39-43</sup> In contrast, in the developing embryonic chicken brain, endoglycan appears to be a negative regulator of cell-cell adhesion during axon guidance and cerebellar Purkinje cell migration.<sup>44</sup> In the kidney, endoglycan is trafficked to the apical surface of developing renal tubules,<sup>38</sup> but whether it contributes to cell adhesion in the kidney in a positive or negative manner, is not yet clear.

Here, we demonstrate that endoglycan is proteolytically shed *in vitro* in mouse neurons and *in vivo* in mouse brains. Using primary murine neurons, we describe the expression pattern of endoglycan in mouse brains, establish endoglycan as an ADAM10 substrate and a positive regulator for neurite branching. Conversely, we demonstrate that ADAM10 has the opposite effect of endoglycan on neurite branching, suggesting that ADAM10-mediated cleavage of endoglycan may contribute to neurite branching.

## 2 | EXPERIMENTAL PROCEDURES

### 2.1 | Expression vectors and antibodies

The expression vector encoding lentiviral supplementary proteins (psPAX2) was a gift from Didier Trono (Addgene plasmid #12260). The expression vector encoding lentiviral envelope protein (pcDNA3.1-VSVG) was described previously.<sup>20</sup> Full-length mouse Endoglycan (PODXL2, UniProt Q8CAE9) was cloned into the BamHI/MluI sites of the pCMV6-Entry mammalian expression vector (Origene) in frame with the C-terminal myc and FLAG tag. Control non-targeting

shRNA and shRNA targeting mouse endoglycan (5'-CCG GGAACATAGACTGTGAAGTATTTCTAGAAATACT TCACAGTCTATGTTCTTTTTGGAAA-3') were cloned into the MluI/EcoRI sites of the pLKO.2-EGFP-WPRE

vector.<sup>20</sup> The lentiviral vector encoding EGFP (pFUGW) was a gift from David Baltimore (Addgene plasmid #14883<sup>45</sup>). The lentiviral vector encoding EGFP-IRES-CRE (pFUGW-Cre) was a gift from Richard L. Haganir

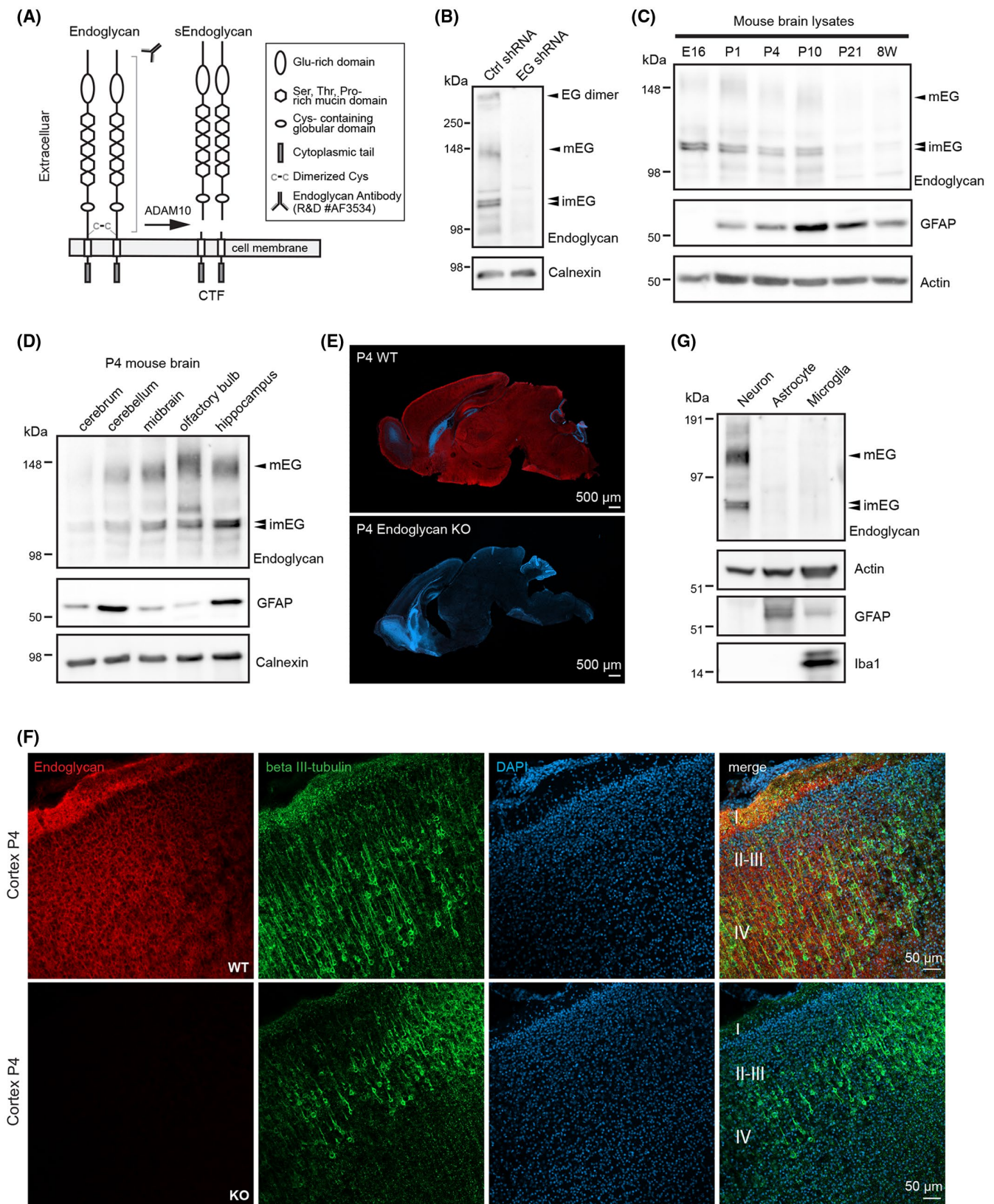


**FIGURE 1** Expression of endoglycan in mouse brain and brain cell types. A, Schematic diagram representing the domain structure of mouse endoglycan. Mouse endoglycan forms homodimers and undergoes ectodomain shedding by ADAM10, releasing the N-terminal soluble endoglycan ectodomain (sEndoglycan) and generating the C-terminal fragment (CTF). The polyclonal antibody used throughout this study (R&D, AF3534) targets the extracellular parts of mouse endoglycan. B, Representative Western blotting results for endoglycan from cultured mouse primary neurons (DIV7). Specific bands for endoglycan (arrowheads) showed reduced signals when endoglycan was lentivirally knocked-down with an endoglycan shRNA as compared to control shRNA. C, Developmental expression profile of endoglycan in mouse brains indicates that endoglycan is developmentally down-regulated. The astrocytic GFAP protein served as a control. D, Spatial expression profile of endoglycan in P4 mouse brains, indicating that endoglycan is expressed higher in, for example, olfactory bulb and midbrain but lower in cerebrum. E, Brain slices from P4 endoglycan WT (upper panel) and littermate KO mice were immunostained for endoglycan (red) and DAPI (blue). No obvious gross morphological difference was observed in the endoglycan KO brain as compared to the WT brain. Signals from endoglycan immunostaining were largely absent in the KO brain, indicating the specificity of the antibody in immunohistochemistry. Scale bars: 500  $\mu\text{m}$ . F, High magnification (10 $\times$ ) of the cortical region from panels E. Cortical layers are indicated as roman numbers (I-IV). Scale bar: 50  $\mu\text{m}$ .  $\beta$  III-tubulin: marker for neurites (green). G, Expression of endoglycan in three major brain cell types. Lysates from primary neurons, astrocytes, and microglia were separated on a MOPS gel, where the molecular weight marker runs differently compared to TRIS gels used in the other panels. Endoglycan showed prominent expression in primary neurons but was largely absent from primary astrocytes and microglia. GFAP and Iba1 were used as markers for astrocytes and microglia, respectively. All experiments shown in this figure have been independently repeated at least two times and similar results were observed. imEG, immature, partially glycosylated endoglycan; mEG, mature, fully glycosylated endoglycan

(The Johns Hopkins University of Medicine). The following primary antibodies were used in this study: endoglycan (0.1  $\mu\text{g}/\text{mL}$ ; R&D, AF3534, targeted against the ectodomain), ADAM10 (1:1000; Abcam, EPR5622),  $\beta$ -actin (1:1000; Sigma, AC-74), Calnexin (1:2000; Enzo Life Sciences, ADI-SPA-860), FLAG (1:2000; Sigma, F7425), Iba1 (1:2000; Wako, 019-19741), GFAP (1:1000; Millipore, EPR1034Y), GluR6/7 (1:1000; Millipore, 04-921), ADAM17 (1:1000; gift from Carl Blobel<sup>46</sup>), and SEZ6 (1:10<sup>47</sup>).

## 2.2 | Mouse strains

The following mouse strains were used in this study: wild type (WT) C57BL/6N (Charles River, Wilmington, MA, USA) or C57BL/6J (in house), ADAM10<sup>f/f</sup>,<sup>48</sup> Endoglycan<sup>f/f</sup>,<sup>38</sup> ADAM17<sup>f/f</sup>,<sup>49</sup> and endoglycan KO mice (see below for the generation of Endoglycan KO mouse line). All animals were maintained with food and water ad libitum and on a 12/12 hours light-dark cycle. All mice were handled in accordance with the European Communities Council Directive (86/609/EEC) and according to institutional guidelines approved by the animal welfare and use committee of the government of Upper Bavaria and housed in standard cages in a specific pathogen-free facility.

## 2.3 | Generation of endoglycan knockout mice

Endoglycan knockout (KO) mice were generated by CRISPR/Cas9-assisted gene editing in zygotes as described previously.<sup>50</sup> Briefly, pronuclear stage zygotes were obtained by mating C57BL/6J males with

superovulated C57BL/6J females. Embryos were then microinjected into the male pronucleus with an injection mix containing four endoglycan-specific CRISPR/Cas9 ribonucleoprotein (RNP) complexes. RNPs consisted of 30 ng/ $\mu\text{L}$  Cas9 protein, 0.15  $\mu\text{M}$  of each crRNA and 0.6  $\mu\text{M}$  tracrRNA (IDT). Protospacer sequences were CTGCTCGCAACCAGTTCCAG and TGC GAGCAGCTA TGAGATCT in intron 2-3, and TGAAGCAGCACCTACCA CTT and AGAGTCCTAGAGTTTTAAGT in intron 4-5. After microinjection, zygotes were cultured in KSOM medium until transferred into pseudopregnant CD-1 foster animals. A mutant founder carrying a 1746 bp deletion (spanning exons 3 & 4) was crossed to a C57BL/6J animal to isolate the knockout allele. To identify putative off target sites of the *Podxl2*-specific crRNAs, the CRISPOR online tool<sup>51</sup> was used and thirteen predicted sites (CFD score >0.6 and MIT score >1.4) were chosen for off-target analysis. Genomic DNA of wildtype and heterozygous mutant mice was isolated and predicted loci were PCR amplified with primers flanking the putative cut sites, and subsequently, Sanger sequenced using the PCR primers. Animals without off-target mutations were used for the generation of the final endoglycan KO line.

## 2.4 | Primary mouse cortical or hippocampal neurons

Hippocampi or cortices from embryonic (E15.5-E16.5) mice were collected and incubated in a digestion medium (DMEM containing 200 U papain and 1 mg/mL L-cysteine, pH 7.4) at 37°C for 20 minutes. Digested tissues were then mechanically dissociated in plating medium (DMEM containing 10% FBS and 1% pen/strep) and plated on 6-well plate or glass coverslips coated with 25  $\mu\text{g}/\text{mL}$  of poly-D-lysine at a density of 1 500 000 cells per

well/6-well plate or 100 000 cells per well/12-well plate. Two-four hours after plating, medium was exchanged to Neurobasal medium (Gibco) supplemented with B27 (Gibco), 1% pen/strep, and 5 mM GlutaMAX (Gibco). Neurons were maintained at 37°C in a cell culture incubator with 5% CO<sub>2</sub> before harvesting or fixation.

## 2.5 | Lentivirus production and infection of primary neurons

Lentiviral particles were generated and purified as previously described.<sup>18,52</sup> Briefly, plasmids encoding lentiviral helper proteins (psPAX2), an envelope protein (pcDNA3.1-VSVG) and gene-of-interest in lentiviral transfer vector were co-transfected in HEK293T cells (maintained in DMEM + 10% FCS, 100 µg/mL G418) using Lipofectamine 2000 following the manufacturer's instructions. 24 hours after transfection, the medium of transfected HEK293T cells was exchanged into packaging medium (DMEM + 2% FCS, 10 mM sodium butyrate) and the conditioned medium was collected 48 hours after transfection. Lentiviral particles were then purified by ultracentrifugation (22000 rpm for 2 hours at 4°C in SW40 rotor, Beckman Coulter). Primary neurons were infected with lentivirus at DIV1.

## 2.6 | Western blotting

Whole-cell lysates were prepared with the STET lysis buffer (50 mM Tris-HCl pH 7.5, 150 mM NaCl, 1 mM EDTA, 1% Triton X-100, protease inhibitors cocktail). To detect the soluble form of endoglycan (sEndoglycan), 48 hours conditioned media from 1.5 million primary cortical neurons were collected and enriched with Concanavalin A (ConA) beads (Sigma, Merck, Darmstadt, Germany; C7555). Briefly, 1 mL of conditioned medium was incubated with 20 µL of ConA beads pre-equilibrated with ConA wash buffer (20 mM Tris-HCl pH 7.5, 500 mM NaCl, 1 mM CaCl<sub>2</sub>, 1 mM MnCl<sub>2</sub>) overnight at 4°C with rotation, and then washed two times with ConA wash buffer before adding the 4× Laemmli buffer with 10% β-mercaptoethanol. Samples were boiled for 5 minutes at 95°C before separation with SDS-PAGE on 8% or 10% Tris-glycine gels, 8%-20% gradient MOPS gels (Genscript). Afterward, samples were transferred to Nitrocellulose (NC) membranes, blocked with 5% skim milk, and incubated with primary antibody overnight at 4°C, followed by HRP-conjugated secondary antibody for 1 hours at RT. Proteins were visualized with ECL on an ImageQuant system (GE Healthcare).

## 2.7 | Mouse brain homogenization

Brains were isolated from WT mice at different ages and homogenized in STET buffer (50 mM Tris-HCl pH 7.5, 150 mM NaCl, 1 mM EDTA, 1% Triton X-100, protease inhibitors cocktail) with a Teflon homogenizer. Samples were incubated on ice for at least 30 minutes and centrifuged at maximum speed for 10 minutes at 4°C in order to remove the Triton X-100 insoluble fraction. BCA assay (Uptima Interchim, UP95425) was used to quantify protein concentrations and 15-20 µg of total protein were used for western blot analysis.

## 2.8 | Immunohistochemistry of mouse brains

Male and female postnatal (P4) mouse pups were used for the collection of brain tissue either expressing or lacking endogenous endoglycan. Animals were sacrificed by decapitation and tail biopsies were taken for genotyping. Brains were removed and washed in 0.1 M phosphate-buffered saline (PBS) and immersion fixed in 4% paraformaldehyde (PFA) overnight. For cryopreservation brains were then stored in 20% sucrose in 0.1 M PBS until use at 4°C. For cutting, brains were embedded in optimal cutting temperature compound (Tissue-Tek O.C.T., Sakura), frozen on dry ice and kept at -80°C until sectioning. 30 µm sagittal brain sections were cut using a cryostat at -20°C (CryoSTAR NX70 Kryostat, Thermo Scientific). Free-floating sections were collected first in PBS to avoid contamination of the O.C.T. cube with storage solution. Sections were then transferred into a storage solution (25 % Glycerin, 25% Ethylene Glycol in 0.1 M PBS) and stored at 4°C until staining. Briefly, free-floating sections were blocked and permeabilized with blocking solution (0.03% TritonX-100, 10% horse serum, 5% sucrose and 2% bovine serum albumin (BSA) in 0.1 M PBS) for 1 hour at room temperature (RT). Subsequently, sections were incubated overnight at 4°C in antibody solution (5% BSA in 0.1 M PBS) with the following primary antibodies: Endoglycan/PODXL2 (1:1000, AF3534, R&D System) and β-Tubulin-III (1:500, T3952, Sigma Aldrich). After primary antibody incubation, brain sections were washed with PBS three times and incubated with appropriate fluorophore-conjugated secondary antibodies (Donkey anti-Goat, Alexa Fluor 555 [1:1000, A21202, Invitrogen]; Donkey anti-Rabbit, Alexa Fluor 488 [1:1000, A21206, Invitrogen]) together with the nuclear stain DAPI (1:1000, D8417-IMG, Sigma-Aldrich) for one hour in the dark at RT. Sections were afterward washed three times with PBS, mounted onto glass slides

(Thermo Scientific), dried in the dark for at least one hour and mounted using Fluoroshield (Sigma-Aldrich). Expression patterns of endoglycan were then imaged by confocal microscopy (Zeiss LSM 900 Aryscan2).

## 2.9 | Image acquisition

Representative images of P4 endoglycan wild type and knockout mouse brains were taken to demonstrate expression patterns of endoglycan of at least four mice per genotype. To show an overview of the sagittal sections and the expression patterns, overview tile images were acquired using a confocal microscope (2.5×, 12 tiles, Zeiss LSM 900 Airyscan2). For detailed images, four regions of interest (ROI) were selected: Isocortex, Hippocampus, Cerebellum, Olfactory Bulb. For each ROI images in 10× magnification were taken. Images were latterly edited using ImageJ software.

## 2.10 | Mouse brain fractionation

To isolate the soluble and membrane fractions of mouse brains, brains isolated from P14 WT and endoglycan KO mice were homogenized in DEA buffer (50 mM NaCl, 2 mM EDTA, 0.2% Diethylamine, protease inhibitors cocktail) with a Teflon homogenizer and the homogenates were quickly neutralized with 0.1 volume of neutralization buffer (0.5 M Tris-HCl pH 6.8). The homogenates were then centrifuged at 4000×g for 5 minutes at 4°C. The pellets were washed twice with PBS (after each wash centrifugation at 4000×g for 5 minutes at 4°C) and the membrane fraction was obtained by extraction with the STET buffer (50 mM Tris-HCl pH 7.5, 150 mM NaCl, 1 mM EDTA, 1% Triton X-100, protease inhibitors cocktail). To obtain the soluble fraction, the supernatant after the initial centrifugation was further ultracentrifuged at 136 000×g for 30 minutes at 4°C. The supernatant after the ultracentrifugation was collected as the soluble fraction. Samples were quantified by BCA assay and analyzed by western blotting.

## 2.11 | Surface biotinylation

Neurons were biotinylated at DIV7 with EZ-Link Sulfo-NHS-Biotin (ThermoFisher, 21217) according to the manufacturer's protocols. Excess biotin reagents were quenched by 100 mM Glycine/PBS. Neurons were lysed with SDS lysis buffer (50 mM Tris-HCl pH 8, 150 mM NaCl, 2 mM EDTA, 1% SDS) and the lysates were cooked at 95°C for 5 minutes followed by dilution with

RIPA buffer (10 mM Tris-HCl pH 8, 150 mM NaCl, 2 mM EDTA, 1% Triton, 0.1% sodium deoxycholate, 0.1% SDS). 80 µg of total lysates were incubated with 10 µL of streptavidin agarose (ThermoFisher, 20361) O/N at 4°C with rotation. Beads were washed with RIPA buffer and the bound proteins were eluted in Laemmli buffer supplemented with 3 mM biotin by boiling at 95°C. Samples were analyzed by Western blotting. Compared to whole lysates, this method reduced cytosolic proteins in the surface fraction as described previously.<sup>47,53</sup>

## 2.12 | Cell-free ADAM10 in vitro cleavage assay

Full-length mouse endoglycan with C-terminal myc and FLAG tag was overexpressed in HEK293T cells using Lipofectamine 2000 following the manufacturer's instructions. 48 hours after the transfection, cell lysates were harvested with STET buffer (50 mM Tris-HCl pH 7.5, 150 mM NaCl, 1 mM EDTA, 1% Triton X-100, protease inhibitors cocktail). The overexpressed endoglycan was immunoprecipitated from the lysates using anti-FLAG M2 beads (Sigma, A2220). The beads were then washed twice with the STET buffer and twice with ADAM10 reaction buffer (25 mM Tris-HCl pH 9.0, 50 µM ZnCl<sub>2</sub>, 0.01% Brij35). The immunoprecipitated full-length mouse endoglycan were then incubated with 0.4 µg of mouse recombinant ADAM10 ectodomain (R&D, 946-AD) in the presence or absence of 5 µM GI254023X (Sigma, SML0789) in the ADAM10 reaction buffer at 37°C for 2 hours. As the no substrate control, immunoprecipitation was performed on non-transfected HEK293T cells lysates. After the incubation with recombinant ADAM10, supernatant (no beads) and bead fractions were separated by centrifugation at 800×g for 2 minutes and the reaction was stopped by adding Laemmli buffer supplemented with β-mercaptoethanol. The samples were then analyzed by western blotting.

## 2.13 | Immunostaining of cultured neurons

For immunostaining of endoglycan and F-actin in cultured mouse neurons, neurons plated on coverslips were fixed with ice-cold methanol at DIV4. To confirm the endoglycan antibody specificity, neurons were infected with lentiviruses encoding control shRNA or mouse endoglycan shRNA at DIV1. Fixed neurons were permeabilized and blocked with 1× PBS containing 10% horse serum, 0.03% TritonX-100, 5% Sucrose, and 2% BSA for 1 hours

at RT. Neurons were then stained with primary antibody against mouse endoglycan (0.1  $\mu\text{g}/\text{mL}$ ; R&D AF3534), and MAP2 (1:1000; Abcam, ab5392), diluted in 5% BSA/PBS at 4°C over night, followed by secondary antibody (donkey anti-goat Alexa 488), rhodamine phalloidin (1:500; Cytoskeleton Inc., #PHDR1, or goat anti-chicken Alexa 594) diluted in 5% BSA/PBS 1 hour at RT. Confocal images were acquired on a Leica SP5 and Zeiss LSM 900 ArysCAN2 microscope.

### 2.14 | Calcium phosphate transfection of primary hippocampal neurons, Sholl analysis and neurite tracing

Cultured hippocampal neurons prepared from ADAM10<sup>f/f</sup>, endoglycan<sup>f/f</sup>, and ADAM17<sup>f/f</sup> mice were transfected with an EGFP expression vector (pFUGW) or an EGFP and Cre co-expression vector (pFUGW-Cre) at DIV1. The calcium phosphate transfection kit (Takada, #631312) was used according to the manufacturer's recommendation. Neurons were fixed at DIV7 with 4% PFA and images were acquired on a Leica SP5 confocal microscopy. Sholl analysis of neurites complexity was performed according to a previous publication<sup>54</sup> with minor modifications. Briefly, images of single neurons were binarized and the Sholl Analysis plugin (v3.4.5) in ImageJ (Fiji) was used for the analysis. Concentric circles were drawn at 10- $\mu\text{m}$  intervals using the cell body as the common center. The starting radius was set at 10  $\mu\text{m}$  and the ending radius was set at 100  $\mu\text{m}$ . Numbers of neurites crossing each of the circles were counted automatically. Neurons were chosen based on the presence of continuous and extended neurites without unusual blebbing, and were excluded when neurites circling around the soma because this morphology confounds the analysis. The neurites were traced by NeuronJ plugin in imageJ(Fiji) software for manual tracing as previously described.<sup>55,56</sup> Acquisition and analyses of images were done by a blind observer.

### 2.15 | Statistics

GraphPad Prism was used for statistical analysis. For comparison between two samples, an unpaired *t*-test was used and  $P < .05$  was considered as statistically significant. For comparison between more than two samples, one-way ANOVA followed by Tukey's post hoc test was used and  $P < .05$  was considered as statistical significant. All replicates used in statistical analysis were prepared from at least two independent experiments. For qualitative results, the same experiments were performed at least two times independently and similar results were observed.

## 3 | RESULTS

### 3.1 | Expression of endoglycan in neurons and mouse brain

To detect endoglycan in neurons and brain, a polyclonal antiserum raised against the ectodomain of endoglycan was used (Figure 1A).<sup>38</sup> In immunoblots of primary neuron lysates several bands were detected at different apparent molecular weights (Figure 1B). Most of the bands were specific for endoglycan because their intensity was strongly reduced upon lentiviral knock-down of endoglycan with shRNAs (Figure 1B). The most intensive bands were a double band at around 105 kDa (immature EG, imEG) and a broad band at around 140 kDa (mature EG, mEG). This is in agreement with previous studies using other cell types that demonstrated that endoglycan is intensively glycosylated within its ectodomain, including N-glycosylation, O-glycosylation and chondroitin sulfate glycosamino-glycan (CS-GAG) modifications.<sup>35,36</sup> An additional broad band was seen at >250 kDa (EG dimer). This may be a homodimer of endoglycan, because endoglycan has a single unpaired cysteine close to its transmembrane domain (Figure 1A)<sup>35</sup> that is known to cause endoglycan dimerization.<sup>36</sup>

Because endoglycan has not yet been investigated in the mammalian brain, we next analyzed its expression in mouse brain across different developmental stages, in different mouse brain areas and in different mouse brain cell types. Endoglycan expression was high in late embryogenesis and early after birth, but dropped sharply between the second and third postnatal week and remained low in adult brain (Figure 1C). When analyzing primary neurons prepared at embryonic day 16 (E16), endoglycan expression increased from the first day in vitro (DIV1) to DIV9 (Supplementary Figure S1). At postnatal day 4 (P4), endoglycan was expressed broadly in mouse brain, as seen by immunoblot analysis (Figure 1D) and by immunohistochemistry (Figure 1E,F and Supplementary Figure S2). As a control for the immunohistochemical staining, we generated endoglycan-deficient mice (Endoglycan KO, Podxl2KO) using CRISPR/Cas9-assisted gene editing (Supplementary Figure S3A). Endoglycan KO mice were viable and fertile and were born at a normal Mendelian ratio from matings of heterozygous to heterozygous mice (Supplementary Figure S3B), in agreement with a previous study.<sup>38</sup> No obvious gross morphological difference was observed in the endoglycan KO brain as compared to the WT brain. Signals from endoglycan immunohistostaining were largely absent in the KO brain, indicating the specificity of the antibody in immunohistochemistry (Figure 1E,F, Supplementary Figure S2). Immunohistostaining for endoglycan was also analyzed at higher magnification in

specific brain areas. Expression of endoglycan was seen within the cortical region, especially in layer I (Figure 1F), in the CA1 and CA3 region of the hippocampus (Supplementary Figure S2A, upper panels) and within the molecular layer of the cerebellum (Supplementary Figure S2B, middle panels). In the olfactory bulb, a strong expression of endoglycan was observed in the glomerular layer (GL), but also in the external plexiform layer (EPL) as well as between the mitral cell layer (MCL) and the granule cell layer (GCL) (Supplementary Figure S2C, lower panels). Finally, we found by immunoblot analysis that endoglycan expression was prominent in primary neurons, but largely absent from primary astrocytes and microglia (Figure 1G). Thus, for the next experiments we focused on neuronal endoglycan. Taken together, endoglycan is

broadly expressed in mouse brain with a high expression shortly before and after birth and with a strong expression in neurons.

### 3.2 | Neuronal endoglycan shedding is mediated by ADAM10

Next, we tested whether endoglycan undergoes shedding in primary neurons and whether this is mediated by ADAM10. Neurons from mice with a floxed ADAM10 gene<sup>48</sup> were lentivirally transduced with Cre recombinase to generate ADAM10 knock-out (ADAM10KO) neurons or with GFP to maintain endogenous ADAM10 expression. Deletion of ADAM10 reduced soluble endoglycan

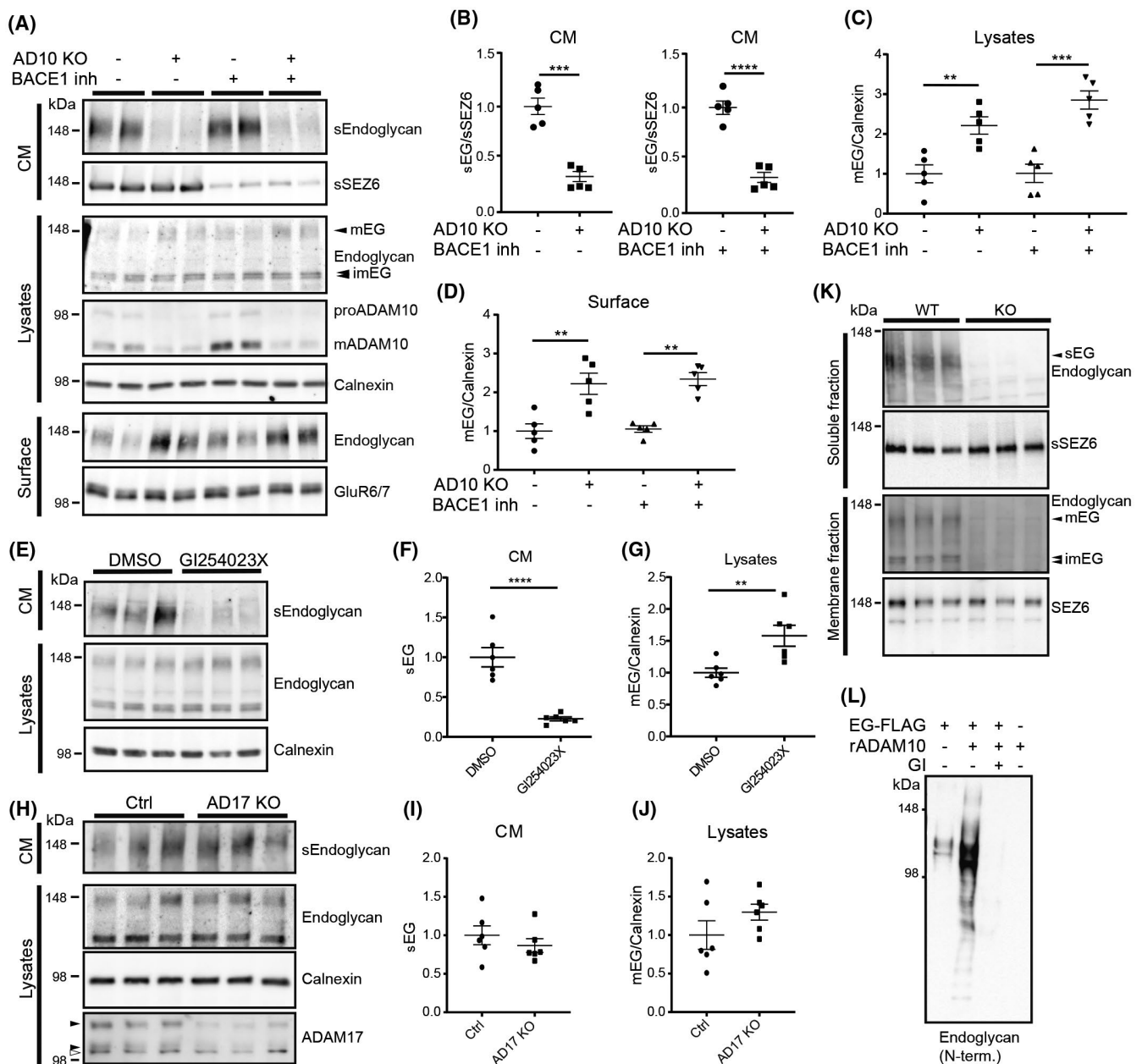




**FIGURE 2** Endoglycan is shed in vitro and in vivo and is a direct substrate of ADAM10. A, Primary neurons were prepared from ADAM10<sup>fl/fl</sup> mice, lentivirally transduced with control virus (Ctrl) or Cre-expressing virus (AD10KO), and treated with DMSO or BACE inhibitor (BACE1 inh). Conditioned media (CM), lysates, and surface proteins enriched with surface biotinylation were collected at DIV7 and analyzed by Western blotting. Reduction of ADAM10 in the ADAM10KO neurons was confirmed by ADAM10 western blotting in lysates. Levels of soluble endoglycan ectodomain (sEndoglycan) released into the CM were dramatically reduced by AD10KO but not by BACE1 inhibitor treatment, indicating endoglycan is an ADAM10 substrate but not a BACE1 substrate. The reduced shedding of endoglycan by ADAM10 was accompanied by a concomitant increase of full-length, mature endoglycan (mEG) in the lysates and on the neuronal surface. Soluble SEZ6 (sSEZ6), generated by BACE1, but not by ADAM10, was used as a positive control for BACE1 inhibitor treatment and additionally demonstrates that ADAM10 knock-out does not alter the shedding of a non-ADAM10 substrate. Calnexin and GluR6/7 were used as loading controls for lysates and surface proteins, respectively. mEG: mature, fully glycosylated endoglycan; imEG: immature, partially glycosylated endoglycan. B-D, Quantification of results in A. Protein abundance of sEndoglycan (sEG) was normalized for sSEZ6. Results were analyzed by unpaired *t*-test (B) or one-way ANOVA followed by Tukey's multiple comparisons test (C, D). E, WT primary neurons were treated with DMSO or 5  $\mu$ M of the ADAM10 inhibitor GI254023X at DIV5. Samples were collected at DIV7. GI254023X treatment reduced sEG levels in CM and increased full-length endoglycan levels in lysates. F,G, Quantification results for E. Results were analyzed by unpaired *t*-test. H, Primary neurons were prepared from ADAM17<sup>fl/fl</sup> mice and lentivirally transduced with control virus (Ctrl) or Cre-expressing virus (AD17KO). Reduction of ADAM17 was confirmed by ADAM17 western blotting in lysates. Closed arrowheads indicate specific bands for ADAM17 and the unspecific band is indicated by an opened arrowhead. Both sEG levels in CM and full-length Endoglycan levels in lysates were not altered in AD17KO, indicating that endoglycan is not an ADAM17 substrates in primary neurons under constitutive condition. I,J, Quantification results for H. Results were analyzed by unpaired *t*-test. K, P14-old endoglycan KO and littermate WT mouse brains were fractionated into membrane and soluble fractions. The detection of endoglycan with the N-terminal antibody in the soluble fraction indicates that endoglycan also undergoes shedding in vivo. L, Cell-free in vitro cleavage assay for endoglycan and ADAM10. Full-length endoglycan with a C-terminal FLAG tag (EG-FLAG) was overexpressed in HEK293T cells and immunoprecipitated with anti-FLAG agarose beads, which were incubated with recombinant ADAM10 in the presence or absence of the ADAM10 inhibitor GI254023X (GI, 5  $\mu$ M). The supernatant fractions (no anti-FLAG beads), which may contain shed soluble endoglycan, were resolved on a tris gel and immunoblotted for endoglycan (N-terminal). The shed endoglycan was only detected when full-length endoglycan was incubated with active ADAM10

levels in the neuronal conditioned medium by 67% (Figure 2A,B), demonstrating that endoglycan is a likely substrate for ADAM10. Of note, the reduced amount of soluble endoglycan in the conditioned medium was accompanied by an increased level of mature, full length endoglycan in the lysates and at the neuronal cell surface (Figure 2A,C,D), suggesting that ADAM10-deficiency may increase a potential cell-surface function of full-length endoglycan. As a control, we verified that the shed form (sSEZ6) of seizure protein 6 (SEZ6), which is not related to endoglycan and not cleaved by ADAM10, but by BACE1,<sup>47,53</sup> was not affected by ADAM10-deficiency (Figure 2A). We also treated primary neurons with the BACE1 inhibitor C3.<sup>57</sup> As expected, C3 did not block shedding of endoglycan, but of SEZ6 (Figure 2A).

Of note, the apparent molecular weight of the shed endoglycan was similar to the full-length, mature, membrane-bound endoglycan at around 148 kDa. As a result of the membrane-proximal shedding event, the shed endoglycan is expected to lack the C-terminal approximately 110 amino acids comprising the transmembrane and the short cytoplasmic domain of full-length endoglycan (Figure 1A). Given the large molecular weight of the highly glycosylated endoglycan ectodomain, the molecular weight difference of about 11 kDa may not be easily resolved by immunoblot analysis. The finding that only the mature, 148 kDa endoglycan, but not the immature 105 kDa form is shed, is consistent with other ADAM10

substrates, such as APP<sup>20,21</sup> and with the cellular localization of active ADAM10, which is assumed to cleave its substrates late in the secretory pathway or at the plasma membrane.

In addition to the genetic deletion of ADAM10, a pharmacological approach was applied, where wild-type neurons were treated with the ADAM10-preferring metalloprotease inhibitor GI254023X.<sup>58</sup> Similar to the ADAM10-deficiency, inhibition of ADAM10 strongly reduced endoglycan shedding by 77% (Figure 2E-G). As a control experiment we deleted the close ADAM10-homolog ADAM17 with Cre in neurons with a floxed ADAM17 gene.<sup>49</sup> While Cre reduced ADAM17 levels, it did not affect levels of shed endoglycan in the conditioned medium or levels of full-length endoglycan in the lysates, demonstrating that under physiological conditions endoglycan in neurons is shed by ADAM10, but not by ADAM17 (Figure 2H-J).

Shedding of endoglycan was also observed in vivo in mouse brains which were collected at P14 and fractionated with diethylamine (DEA) into a soluble and a membrane fraction. Soluble endoglycan was detected in the soluble fraction of wild-type, but not of endoglycan KO mouse brains (Figure 2K), demonstrating that endoglycan undergoes shedding in vivo in mouse brains.

Next, we used a cell-free in vitro assay to test whether recombinant endoglycan can be directly cleaved by recombinant ADAM10. To this aim, a C-terminal FLAG epitope tag was added to endoglycan. The protein was

expressed in human embryonic kidney 293T (HEK293T) cells and immunoprecipitated with anti-FLAG agarose beads. Upon addition of ADAM10 soluble endoglycan was released from the beads (Figure 2L).

Taken together, we conclude from the cellular and cell-free experiments that endoglycan undergoes shedding *in vitro* and *in vivo* and is a direct substrate of ADAM10.

### 3.3 | Endoglycan localizes to neuronal growth cones and controls neurite branching in hippocampal neurons *in vitro*

Endoglycan may act as a cell adhesion protein in axon guidance and cell migration in the chicken brain.<sup>44</sup> In the mammalian nervous system, endoglycan has not yet been studied. One instance where a tight control of cell adhesion is important, is during branching of neurites that extend from the neuronal soma, which is required for correct synapse formation. To determine whether endoglycan is found along neurites, we used

immunocytochemistry of cultured primary neurons. Endogenous endoglycan was observed in the soma and along the neurites, where it colocalized with MAP2, a dendritic marker, and was also found in the growth cone (Figure 3A,B, Supplementary Figure S4), which is the F-actin-rich widening tip of the growing neurite (Figure 3B), where actin and endoglycan showed partial colocalization (Figure 3B).

To test for a potential role of endoglycan in neurite branching, hippocampal neurons were prepared from previously established conditional endoglycan-deficient mice (*endoglycan<sup>fl/fl</sup>*,<sup>38</sup>). Lentiviral Cre recombinase transduction achieved a strong reduction of endoglycan protein levels (Figure 4A) compared to control-transduced neurons, demonstrating an efficient knock-out (Figure 4A). The advantage of using conditional knock-out neurons is that control and knock-out neurons are from the same neuronal preparation, which ensures that potential changes in neurite branching result specifically from the loss of endoglycan but not from potential differences in the preparation of wild-type and knock-out neurons. To investigate whether

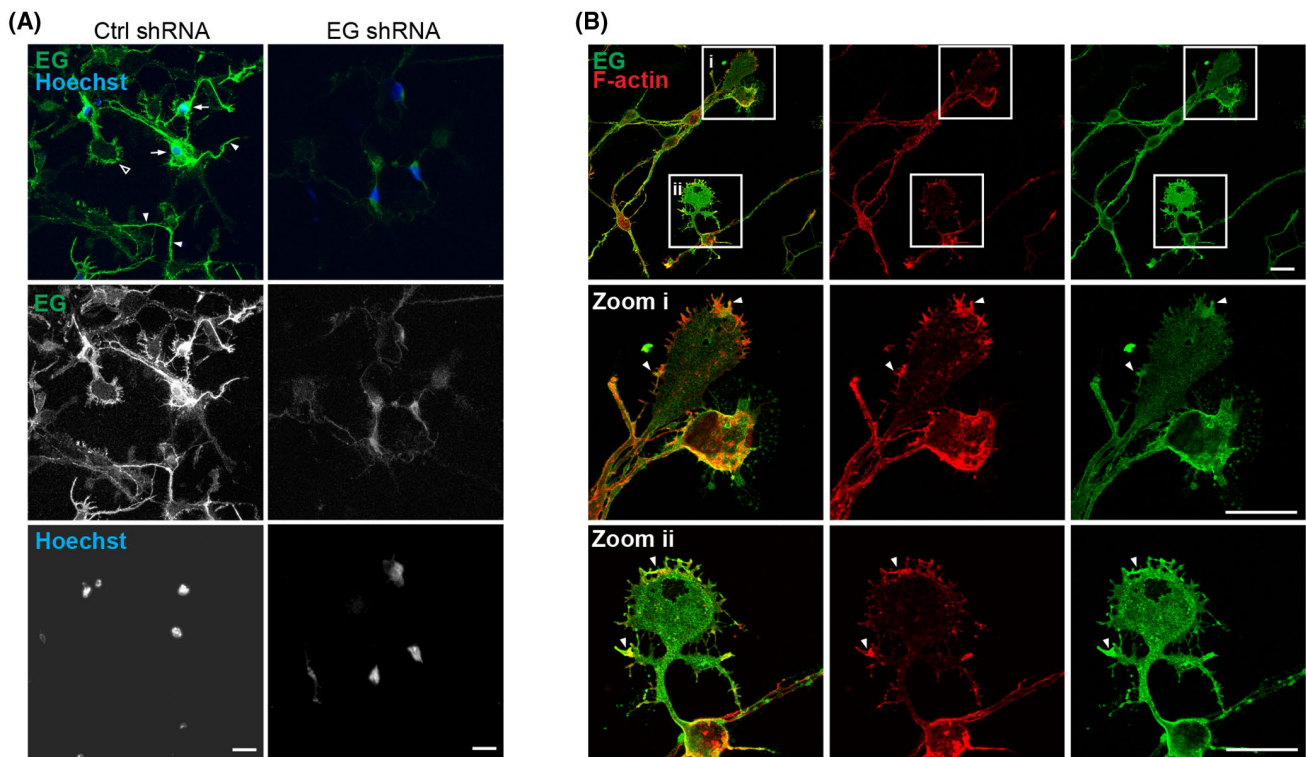


**FIGURE 3** Subcellular localization of endoglycan in primary neurons. A, Immunostaining of endoglycan on mouse primary neurons at DIV4. Endoglycan shRNA was used as a negative control for the antibody specificity. Neurons transduced with control shRNA showed endoglycan-positive staining in neuronal somata (arrows), neurites (filled arrowheads) and in the growth cone-like structure (open arrowhead). Scale bars, 25  $\mu$ m. B, Endoglycan colocalized with F-actin in the neuronal growth cones (arrowheads). Co-staining of endoglycan with phalloidin to label F-actin in neuronal growth cones in primary neurons at DIV4. High magnification in white boxes labelled in the upper panels were shown in the middle and lower panels. Scale bars, 25  $\mu$ m

endoglycan affects neurite branching, hippocampal neurons were sparsely transfected with GFP (control) or with GFP-IRES-CRE (endoglycan KO) at DIV1. The sparse labeling with GFP allows tracing of neurites and

their origin from one specific soma. At DIV7 neurons were fixed, imaged by confocal microscopy and analyzed for changes in neurite branching using the established Sholl method.<sup>54</sup> To this aim, concentric circles

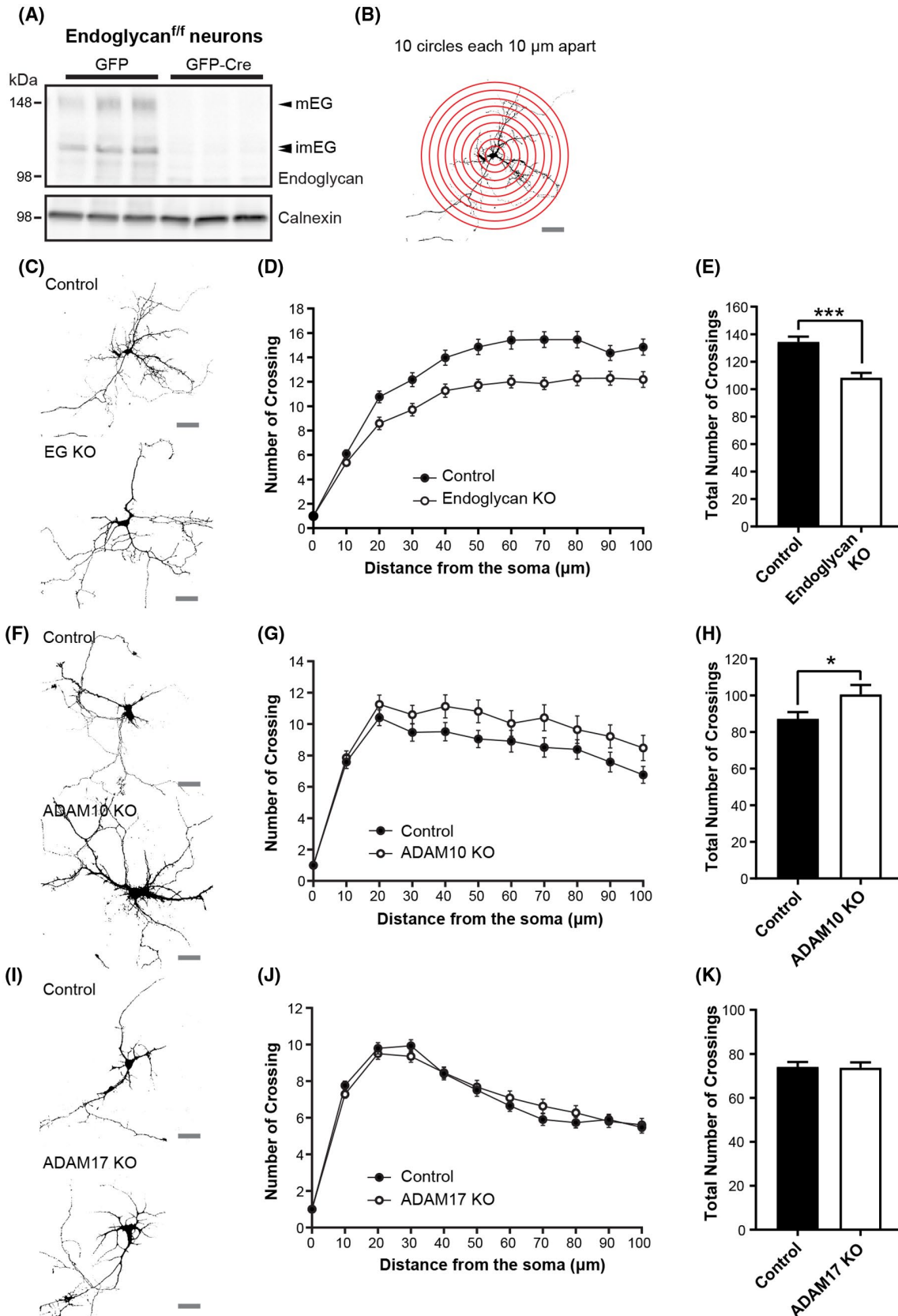


**FIGURE 4** Deficiency of endoglycan reduced neurite branching in vitro. A, Primary neurons were prepared from Endoglycan<sup>fl/fl</sup> mice at E15.5/E16.5 and lentivirally transduced with a GFP construct or a GFP and Cre co-expressing construct (GFP-Cre) at DIV1. Neuronal lysates were prepared at DIV7 and immunoblotted for endoglycan. Neurons transduced with GFP-Cre showed nearly absent endoglycan levels, validating the endoglycan-deficiency model in vitro. Calnexin was used as a loading control. B, Model of the standard Sholl analysis used. The interceptions of the dendrites with 10 circles, which are 10  $\mu\text{m}$  apart and centred around the soma of the neuron were counted. C,F,I, Representative pictures of neurons for the Sholl analysis. Hippocampal neurons were prepared from endoglycan<sup>fl/fl</sup> (C), ADAM10<sup>fl/fl</sup> (F), or ADAM17<sup>fl/fl</sup> mice (I) and transfected with GFP (Control) or GFP-Cre (respective KO) constructs with the calcium phosphate method to sparse label the transfected neurons with GFP. Scale bars, 50  $\mu\text{m}$ . (D,G,J) Sholl analysis profiles of control (N = 63) and Endoglycan KO (N = 66) neurons (D), control (N = 45) and ADAM10 KO (N = 48) neurons (G), and control (N = 162) and ADAM17 KO (N = 168) neurons (J). Neuronal soma was used as the common center and concentric circles were drawn every 10  $\mu\text{m}$  up to a distance of 100  $\mu\text{m}$ . Number of crossings on each circle is plotted against the distance from the soma. E,H,K, Total number of crossings from the Sholl profile were used for the statistical analysis. Deficiency of endoglycan reduces neurite branching (E), whereas deficiency of ADAM10 increases neurite branching (H). Deficiency of ADAM17 has no impact on neurite branching (K). Samples were analyzed by unpaired *t*-test. Error bars represent SEM

were drawn at 10- $\mu\text{m}$  intervals using the cell body as the common center (Figure 4B). The number of neurites crossing each of the circles were counted automatically. The number of crossings was significantly lower in Cre-transfected compared to control neurons (Figure 4C-E). This result of decreased neurite branching upon loss of endoglycan demonstrates a new function for endoglycan in inducing neurite branching.

Because we found that ADAM10, but not ADAM17, sheds endoglycan in neurons and that loss of ADAM10 increases cell surface endoglycan levels (Figure 2), we predicted that loss of ADAM10 may increase neurite branching and, thus, would have the opposite effect of the loss of endoglycan on neurite branching. Indeed, loss of ADAM10 significantly increased neurite branching primary hippocampal neurons (Figure 4F-H). In contrast, loss of ADAM17, which did not shed endoglycan and did not have an impact on the level of full-length endoglycan in the lysate (Figure 2), also did not affect neurite branching (Figure 4I-K). Total neurite length and mean neurite length were not altered in the different genotypes compared to the control neurons (Supplementary Figure S5). In summary, these Sholl analyses demonstrate a new role for endoglycan in mediating neurite branching and suggest that endoglycan shedding by ADAM10 is a mechanism to control this function.

## 4 | DISCUSSION

Endoglycan belongs to the CD34-family of highly glycosylated sialomucins and is assumed to have a function in cell adhesion, but little is known about its expression, function and processing in the nervous system. Our study demonstrates that endoglycan is widely expressed in mouse brains and at higher levels in embryonic and newborn compared to adult mouse brains. Endoglycan was found to have a function in neural development in vitro by controlling the process of neurite branching. Finally, this

study reveals that endoglycan is proteolytically processed by ADAM10, a key protease in nervous system development and function.

The new function of endoglycan in neurite branching discovered in our study suggests a role for endoglycan in the development of mouse neurons toward their function in neuronal circuits. This is in line with the high expression of endoglycan before and after birth observed in our study and with a recent in vivo study revealing another neurodevelopmental role for endoglycan in the chicken brain.<sup>44</sup> That study reported that endoglycan negatively regulates cell-cell adhesion during outgrowth and pathfinding of axons (axon guidance) and during the migration of Purkinje cells in the chicken cerebellum. Whether the neurite branching function in our study and the in vivo function in the chicken brain reflect the same cell adhesive molecular function of endoglycan, remains unclear and may require identification of yet unknown endoglycan binding partners or ligands. Neurite branching is essential for normal development, but its mechanisms and the contributing proteins are not fully understood. Interestingly, the endoglycan homolog PODXL is also one of the contributing proteins and has been shown to be specifically required for neurite growth, branching and axonal fasciculation<sup>59</sup> and correct brain anatomy.<sup>60</sup> In contrast to PODXL-deficient mice, which show perinatal lethality,<sup>59</sup> endoglycan-deficient mice are viable and fertile as observed in our and in a previous study.<sup>38</sup> Thus, future studies are required to dissect in detail the molecular functions of endoglycan and its homolog PODXL and to evaluate potential functional complement or overlap between both homologous proteins.

Another key finding of our study is that endoglycan undergoes ectodomain shedding, both in vitro in primary neurons and in vivo in the mouse brains. In addition, when reanalyzing our previous whole-proteome studies of murine and human CSF,<sup>19,53,61</sup> a shed form of endoglycan was detected, demonstrating that endoglycan shedding can also be monitored in body fluids of different organisms. Shedding can occur under non-stimulated conditions,

which is referred to as constitutive shedding.<sup>1</sup> In addition, stimulation of certain cellular signaling pathways, for example, through phorbol esters or neuronal stimulation, may upregulate the shedding of a membrane protein above its constitutive level and this may be mediated by the same protease as under constitutive conditions or by other proteases. This is referred to as the regulated sheddase. One example is the Alzheimer's disease-linked protein APP, which is constitutively shed by ADAM10,<sup>16,20,21</sup> but may additionally be cleaved by ADAM17 and other metalloproteases, if their activity is stimulated or if they are overexpressed.<sup>62</sup> We report that constitutive shedding of endoglycan is mediated by ADAM10 and not ADAM17 in neurons. Whether ADAM17 may act as additional regulated sheddase for endoglycan, is currently unknown. Interestingly, shedding of the endoglycan homolog PODXL may be controlled in a partially different manner. For example, in previous proteomic studies shed PODXL was not detected from cultured neurons or mouse CSF under physiological conditions,<sup>19,53,61</sup> although PODXL is well expressed in neurons.<sup>63</sup> This suggests that PODXL may not be shed at high levels under physiological conditions, at least from neurons. It was reported that in transfected CHO cells, PODXL undergoes shedding, at least upon activation of protein kinase C through the phorbol ester PMA.<sup>64</sup> Thus, the stimulated sheddase for PODXL may be ADAM17, because PMA is frequently used as an activator of ADAM17 in vitro.<sup>65</sup>

Shedding is an essential cellular mechanism to control the abundance and function of membrane proteins.<sup>1</sup> However, for many shedding substrates, including endoglycan, it has not yet been investigated, whether their function is mediated by the full-length transmembrane form of the protein or by one of the cleavage fragments or even by all of them. An example of a protein for which the functional consequences of shedding have been identified, is the B cell maturation antigen (BCMA) that acts as a surface receptor, whereas the shed ectodomain has a decoy receptor function.<sup>66</sup> Another example is neuregulin-1, where shedding by the protease BACE1 is required to release its ectodomain, which in turn acts as a growth factor to stimulate myelination in the nervous system.<sup>67,68</sup> Additionally, it is even possible that the full-length and the shed ectodomain have different physiological functions, as was shown for death receptor 6, another ADAM10 substrate.<sup>18</sup> Our study suggests that the function of endoglycan in neurite branching is mediated by the full-length form and not the shed ectodomain of endoglycan. This is based on the following rationale. Endoglycan-deficiency reduced neurite branching, which may indicate that either full-length endoglycan or its cleavage fragments are required for normal neurite branching. However, deficiency of the endoglycan

sheddase ADAM10 had the opposite phenotype, induced increased neurite branching and enhanced levels of full-length endoglycan at the neuronal surface. If one of the cleavage fragments of endoglycan was relevant for neurite branching, deficiency of endoglycan or ADAM10 should have shown the same phenotype. Another, less likely but plausible possibility is that shed endoglycan has an inhibitory effect on neurite outgrowth. However, given our sparse knock-out of endoglycan in only a few neurons in the in vitro neurite branching experiment, it is very likely that total shed endoglycan levels in that culture were largely not different from the control condition, suggesting that full-length, but not shed endoglycan has the major function in neurite branching. Thus, we propose that shedding by ADAM10 is a mechanism to terminate the function of full-length endoglycan in neurite branching. In this scenario, shed endoglycan may merely act as a decoy protein sequestering potential endoglycan binding partners. Besides endoglycan, numerous additional neuronal ADAM10 substrates, including N-cadherin, have functions during nervous system development, including in neurite branching and outgrowth.<sup>16,17,32</sup> Thus, a knock-out of ADAM10 will not only phenocopy the shedding inhibition of endoglycan, but also of other neuronal ADAM10 substrates, making dissection of the functions of full-length substrates versus cleavage products challenging for ADAM10, also because ADAM10-deficient mice show embryonic lethality.<sup>15</sup>

We see a possible application for shed endoglycan, that is, its use as a biomarker for ADAM10 activity. ADAM10 is considered as a drug target for neurological and psychiatric diseases, such as Alzheimer's, prion and Huntington's disease.<sup>29,30</sup> Given the wealth of neuronal ADAM10 substrates, a pharmacological modulation of ADAM10 activity needs to be carefully controlled. For example, an increase of neuronal APP shedding through ADAM10, for example, with the drug acitretin, is tested to prevent Alzheimer's disease.<sup>31</sup> At the same time, it is highly desirable to not activate other ADAM10 substrates so strongly that side effects occur. This may be achieved by measuring CSF levels of several ADAM10-shed substrate ectodomains besides APP and adjusting the dose accordingly, so that shedding of APP, but ideally not of other ADAM10 substrates, is mildly activated. The general feasibility of this approach was previously shown for the neuronal membrane protein "neural glial-related cell adhesion molecule" (NrCAM), another ADAM10 substrate.<sup>19</sup> While shed APP levels in human CSF were mildly increased with acitretin, shed NrCAM was barely increased in that proteomics CSF study. Importantly, although endoglycan was not mentioned in that CSF study, its shed levels were also not altered upon acitretin treatment.<sup>19</sup>

Taken together, our study demonstrates the expression pattern of endoglycan in the mammalian brain, reveals a new function for endoglycan during neuronal development, establishes endoglycan as a novel ADAM10 substrate and raises the possibility to use shed endoglycan as a biomarker to monitor ADAM10 activity in clinical trials.

## ACKNOWLEDGEMENTS

The authors thank Katrin Moschke and Anna Berghofer for their technical assistance, Benedikt Brücklmeier for providing mouse primary microglia lysates and Alessio Colombo for providing WT brain slices. This work was funded by the Deutsche Forschungsgemeinschaft (DFG, German Research Foundation) under Germany's Excellence Strategy within the framework of the Munich Cluster for Systems Neurology (EXC 2145 SyNergy– ID 390857198), the SFB 870, the research unit FOR2290 and through the BMBF with project PMG-AD, and National Institutes of Health R01DK099478. JT was supported by a Boehringer Ingelheim Fonds (BIF) PhD fellowship.

## CONFLICT OF INTEREST

The authors declare to have no conflict of interest

## AUTHOR CONTRIBUTIONS

H.-E. Hsia and S. F. Lichtenthaler designed research. H.-E. Hsia, J. Tüshaus, L. I. Hofmann, and X. Feng performed research. B. Wefers and W. Wurst generated the endoglycan knockout mouse line. D. Marciano provided the endoglycan<sup>f/f</sup> mouse line. H.-E. Hsia and S. F. Lichtenthaler wrote the paper.

## REFERENCES

- Lichtenthaler SF, Lemberg MK, Flührer R. Proteolytic ectodomain shedding of membrane proteins in mammals—hardware, concepts, and recent developments. *Embo J*. 2018;37:e99456.
- Jones JC, Rustagi S, Dempsey PJ. ADAM proteases and gastrointestinal function. *Annu Rev Physiol*. 2016;78:243-276.
- Drey Mueller D, Uhlig S, Ludwig A. ADAM-family metalloproteinases in lung inflammation: potential therapeutic targets. *Am J Physiol Lung Cell Mol Physiol*. 2015;308:L325-L343.
- Prox J, Rittger A, Saftig P. Physiological functions of the amyloid precursor protein secretases ADAM10, BACE1, and presenilin. *Exp Brain Res*. 2012;217:331-341.
- Bell KF, Zheng L, Fahrenholz F, Cuervo AC. ADAM-10 overexpression increases cortical synaptogenesis. *Neurobiol Aging*. 2008;29:554-565.
- Pliassova A, Lopes JP, Lemos C, Oliveira CR, Cunha RA, Agostinho P. The association of amyloid-beta protein precursor with alpha- and beta-secretases in mouse cerebral cortex synapses is altered in early Alzheimer's disease. *Mol Neurobiol*. 2016;53:5710-5721.
- Lundgren JL, Vandermeulen L, Sandebring-Matton A, et al. Proximity ligation assay reveals both pre- and postsynaptic localization of the APP-processing enzymes ADAM10 and BACE1 in rat and human adult brain. *BMC Neurosci*. 2020;21:6.
- Lundgren JL, Ahmed S, Schedin-Weiss S, et al. ADAM10 and BACE1 are localized to synaptic vesicles. *J Neurochem*. 2015;135:606-615.
- Marcello E, Gardoni F, Mauceri D, et al. Synapse-associated protein-97 mediates alpha-secretase ADAM10 trafficking and promotes its activity. *J Neurosci*. 2007;27:1682-1691.
- Marcello E, Saraceno C, Musardo S, et al. Endocytosis of synaptic ADAM10 in neuronal plasticity and Alzheimer's disease. *J Clin Invest*. 2013;123:2523-2538.
- Brenneman LH, Moss ML, Maness PF. EphrinA/EphA-induced ectodomain shedding of neural cell adhesion molecule regulates growth cone repulsion through ADAM10 metalloprotease. *J Neurochem*. 2014;128:267-279.
- Marcos S, Nieto-Lopez F, Sandonis A, et al. Secreted frizzled related proteins modulate pathfinding and fasciculation of mouse retina ganglion cell axons by direct and indirect mechanisms. *J Neurosci*. 2015;35:4729-4740.
- Hsia HE, Tushaus J, Brummer T, Zheng Y, Scilabra SD, Lichtenthaler SF. Functions of "disintegrin and metalloproteinases (ADAMs)" in the mammalian nervous system. *Cell Mol Life Sci*. 2019;76:3055-3081.
- Saftig P, Lichtenthaler SF. The alpha secretase ADAM10: a metalloprotease with multiple functions in the brain. *Prog Neurobiol*. 2015;135:1-20.
- Hartmann D, de Strooper B, Serneels L, et al. The disintegrin/metalloprotease ADAM 10 is essential for Notch signalling but not for alpha-secretase activity in fibroblasts. *Hum Mol Genet*. 2002;11:2615-2624.
- Jorissen E, Prox J, Bernreuther C, et al. The disintegrin/metalloproteinase ADAM10 is essential for the establishment of the brain cortex. *J Neurosci*. 2010;30:4833-4844.
- Prox J, Bernreuther C, Altmepfen H, et al. Postnatal disruption of the disintegrin/metalloproteinase ADAM10 in brain causes epileptic seizures, learning deficits, altered spine morphology, and defective synaptic functions. *J Neurosci*. 2013;33:12915-12928, 12928a.
- Colombo A, Hsia HE, Wang M, et al. Non-cell-autonomous function of DR6 in Schwann cell proliferation. *EMBO J*. 2018;37:e97390.
- Brummer T, Muller SA, Pan-Montojo F, et al. NrCAM is a marker for substrate-selective activation of ADAM10 in Alzheimer's disease. *EMBO Mol Med*. 2019;11:e9695.
- Kuhn PH, Wang H, Dislich B, et al. ADAM10 is the physiologically relevant, constitutive alpha-secretase of the amyloid precursor protein in primary neurons. *Embo J*. 2010;29:3020-3032.
- Lammich S, Kojro E, Postina R, et al. Constitutive and regulated alpha-secretase cleavage of Alzheimer's amyloid precursor protein by a disintegrin metalloprotease. *Proc Natl Acad Sci USA*. 1999;96:3922-3927.
- Schlepckow K, Kleinberger G, Fukumori A, et al. An Alzheimer-associated TREM2 variant occurs at the ADAM cleavage site and affects shedding and phagocytic function. *EMBO Mol Med*. 2017;9:1356-1365.
- Thornton P, Sevalle J, Deery MJ, et al. TREM2 shedding by cleavage at the H157-S158 bond is accelerated for the Alzheimer's disease-associated H157Y variant. *EMBO Mol Med*. 2017;9:1366-1378.
- Kim M, Suh J, Romano D, et al. Potential late-onset Alzheimer's disease-associated mutations in the ADAM10 gene attenuate {alpha}-secretase activity. *Hum Mol Genet*. 2009;18:3987-3996.

25. Suh J, Choi SH, Romano DM, et al. ADAM10 missense mutations potentiate beta-amyloid accumulation by impairing pro-domain chaperone function. *Neuron*. 2013;80:385-401.
26. Kunkle BW, Grenier-Boley B, Sims R, et al. Genetic meta-analysis of diagnosed Alzheimer's disease identifies new risk loci and implicates Abeta, tau, immunity and lipid processing. *Nat Genet*. 2019;51:414-430.
27. Altmeyen HC, Prox J, Krasemann S, et al. The sheddase ADAM10 is a potent modulator of prion disease. *Elife*. 2015;4:e04260.
28. Vezzoli E, Caron I, Talpo F, et al. Inhibiting pathologically active ADAM10 rescues synaptic and cognitive decline in Huntington's disease. *J Clin Invest*. 2019;129:2390-2403.
29. Wetzel S, Seipold L, Saftig P. The metalloproteinase ADAM10: a useful therapeutic target? *Biochim Biophys Acta Mol Cell Res*. 2017;1864:2071-2081.
30. Marcello E, Borroni B, Pelucchi S, Gardoni F, Di Luca M. ADAM10 as a therapeutic target for brain diseases: from developmental disorders to Alzheimer's disease. *Expert Opin Ther Targets*. 2017;21:1017-1026.
31. Endres K, Fahrenholz F, Lotz J, et al. Increased CSF APPs-alpha levels in patients with Alzheimer disease treated with acitretin. *Neurology*. 2014;83:1930-1935.
32. Kuhn PH, Colombo AV, Schusser B, et al. Systematic substrate identification indicates a central role for the metalloprotease ADAM10 in axon targeting and synapse function. *Elife*. 2016;5:e12748.
33. Muller SA, Scilabra SD, Lichtenthaler SF. Proteomic substrate identification for membrane proteases in the brain. *Front Mol Neurosci*. 2016;9:96.
34. Nielsen JS, McNagny KM. Novel functions of the CD34 family. *J Cell Sci*. 2008;121:3683-3692.
35. Sassetti C, Van Zante A, Rosen SD. Identification of endoglycan, a member of the CD34/podocalyxin family of sialomucins. *J Biol Chem*. 2000;275:9001-9010.
36. Fieger CB, Sassetti CM, Rosen SD. Endoglycan, a member of the CD34 family, functions as an L-selectin ligand through modification with tyrosine sulfation and sialyl Lewis x. *J Biol Chem*. 2003;278:27390-27398.
37. Leppanen A, Parviainen V, Ahola-Iivari E, Kalkkinen N, Cummings RD. Human L-selectin preferentially binds synthetic glycosulfopeptides modeled after endoglycan and containing tyrosine sulfate residues and sialyl Lewis x in core 2 O-glycans. *Glycobiology*. 2010;20:1170-1185.
38. Yang Z, Zimmerman SE, Tsunozumi J, et al. Role of CD34 family members in lumen formation in the developing kidney. *Dev Biol*. 2016;418:66-74.
39. Sarangapani KK, Yago T, Klopocki AG, et al. Low force decelerates L-selectin dissociation from P-selectin glycoprotein ligand-1 and endoglycan. *J Biol Chem*. 2004;279:2291-2298.
40. Barsegov V, Thirumalai D. Dynamic competition between catch and slip bonds in selectins bound to ligands. *J Phys Chem B*. 2006;110:26403-26412.
41. Tan PC, Furness SG, Merckens H, et al. Na<sup>+</sup>/H<sup>+</sup> exchanger regulatory factor-1 is a hematopoietic ligand for a subset of the CD34 family of stem cell surface proteins. *Stem Cells*. 2006;24:1150-1161.
42. Kerr SC, Fieger CB, Snapp KR, Rosen SD. Endoglycan, a member of the CD34 family of sialomucins, is a ligand for the vascular selectins. *J Immunol*. 2008;181:1480-1490.
43. Sarangapani KK, Marshall BT, McEver RP, Zhu C. Molecular stiffness of selectins. *J Biol Chem*. 2011;286:9567-9576.
44. Baeriswyl T, Dumoulin A, Schaettin M, et al. Endoglycan plays a role in axon guidance by modulating cell adhesion. *Elife*. 2021;10:e64767.
45. Lois C, Hong EJ, Pease S, Brown EJ, Baltimore D. Germline transmission and tissue-specific expression of transgenes delivered by lentiviral vectors. *Science*. 2002;295:868-872.
46. Li X, Maretzky T, Weskamp G, et al. iRhoms 1 and 2 are essential upstream regulators of ADAM17-dependent EGFR signaling. *Proc Natl Acad Sci USA*. 2015;112:6080-6085.
47. Pignoni M, Hsia HE, Hartmann J, et al. Seizure protein 6 controls glycosylation and trafficking of kainate receptor subunits GluK2 and GluK3. *EMBO J*. 2020;39:e103457.
48. Gibb DR, El Shikh M, Kang DJ, et al. ADAM10 is essential for Notch2-dependent marginal zone B cell development and CD23 cleavage in vivo. *J Exp Med*. 2010;207:623-635.
49. Horiuchi K, Kimura T, Miyamoto T, et al. Cutting edge: TNF-alpha-converting enzyme (TACE/ADAM17) inactivation in mouse myeloid cells prevents lethality from endotoxin shock. *J Immunol*. 2007;179:2686-2689.
50. Wefers B, Bashir S, Rossius J, Wurst W, Kuhn R. Gene editing in mouse zygotes using the CRISPR/Cas9 system. *Methods*. 2017;121-122:55-67.
51. Haeussler M, Schonig K, Eckert H, et al. Evaluation of off-target and on-target scoring algorithms and integration into the guide RNA selection tool CRISPOR. *Genome Biol*. 2016;17:148.
52. Rudan Njavro J, Klotz J, Dislich B, et al. Mouse brain proteomics establishes MDGA1 and CACHD1 as in vivo substrates of the Alzheimer protease BACE1. *Faseb J*. 2020;34:2465-2482.
53. Pignoni M, Wangren J, Kuhn PH, et al. Seizure protein 6 and its homolog seizure 6-like protein are physiological substrates of BACE1 in neurons. *Mol Neurodegener*. 2016;11:67.
54. Hsia HE, Kumar R, Luca R, et al. Ubiquitin E3 ligase Nedd4-1 acts as a downstream target of PI3K/PDEN-mTORC1 signaling to promote neurite growth. *Proc Natl Acad Sci USA*. 2014;111:13205-13210.
55. Meijering E, Jacob M, Sarria JC, Steiner P, Hirling H, Unser M. Design and validation of a tool for neurite tracing and analysis in fluorescence microscopy images. *Cytometry A*. 2004;58:167-176.
56. Meijering E. Neuron tracing in perspective. *Cytometry A*. 2010;77:693-704.
57. Stachel SJ, Coburn CA, Steele TG, et al. Structure-based design of potent and selective cell-permeable inhibitors of human beta-secretase (BACE-1). *J Med Chem*. 2004;47:6447-6450.
58. Ludwig A, Hundhausen C, Lambert MH, et al. Metalloproteinase inhibitors for the disintegrin-like metalloproteinases ADAM10 and ADAM17 that differentially block constitutive and phorbol ester-inducible shedding of cell surface molecules. *Comb Chem High Throughput Screen*. 2005;8:161-171.
59. Vitureira N, Andres R, Perez-Martinez E, et al. Podocalyxin is a novel polysialylated neural adhesion protein with multiple roles in neural development and synapse formation. *PLoS One*. 2010;5:e12003.
60. Nowakowski A, Alonso-Martín S, González-Manchón C, et al. Ventricular enlargement associated with the

- panneural ablation of the podocalyxin gene. *Mol Cell Neurosci.* 2010;43:90-97.
61. Tüshaus J, Müller SA, Kataka ES, et al. An optimized quantitative proteomics method establishes the cell type-resolved mouse brain secretome. *Embo J.* 2020;39:e105693.
  62. Asai M, Hattori C, Szabo B, et al. Putative function of ADAM9, ADAM10, and ADAM17 as APP alpha-secretase. *Biochem Biophys Res Commun.* 2003;301:231-235.
  63. Sharma K, Schmitt S, Bergner CG, et al. Cell type- and brain region-resolved mouse brain proteome. *Nat Neurosci.* 2015;18:1819-1831.
  64. Fernandez D, Larrucea S, Nowakowski A, Pericacho M, Parrilla R, Ayuso MS. Release of podocalyxin into the extracellular space. Role of metalloproteinases. *Biochim Biophys Acta.* 2011;1813:1504-1510.
  65. Lorenzen I, Lokau J, Korpys Y, et al. Control of ADAM17 activity by regulation of its cellular localisation. *Sci Rep.* 2016;6:35067.
  66. Laurent SA, Hoffmann FS, Kuhn PH, et al. gamma-Secretase directly sheds the survival receptor BCMA from plasma cells. *Nat Commun.* 2015;6:7333.
  67. Willem M, Garratt AN, Novak B, et al. Control of peripheral nerve myelination by the beta-secretase BACE1. *Science.* 2006;314:664-666.
  68. Hu X, Hicks CW, He W, et al. Bace1 modulates myelination in the central and peripheral nervous system. *Nat Neurosci.* 2006;9:1520-1525.

## SUPPORTING INFORMATION

Additional Supporting Information may be found online in the Supporting Information section.

**How to cite this article:** Hsia H-E, Tüshaus J, Feng X, et al. Endoglycan (PODXL2) is proteolytically processed by ADAM10 (a disintegrin and metalloprotease 10) and controls neurite branching in primary neurons. *FASEB J.* 2021;35:e21813. <https://doi.org/10.1096/fj.20210475R>